SSRG International Journal of Recent Engineering Science
ISSN: 2349–7157 / https://doi.org/10.14445/23497157/IJRES-V11I4P102

Volume 11 Issue 4, 9-15, Jul-Aug 2024

Original Article

Technological and Economic Analysis on Modification of Turbine Shafts and Blades in Geothermal

Sri Wuryanti[1*], G. I. Anggadewi[1]

[1]*Department of Energy Conversion Engineering, Politeknik Negeri Bandung, Bandung, Indonesia.*

[*]*Corresponding Author : sriwuryanti.lamda@gmail.com*

Received: 12 May 2024 Revised: 24 June 2024 Accepted: 13 July 2024 Published: 02 August 2024

Abstract *- The 55 MW geothermal power plant has been operating for 35 years. This generator experienced a reduction in turbine efficiency from 0.88 to 0.56. The decrease in turbine efficiency resulted in an increase in the volume of steam, a decrease in the power produced by the turbine, and instability in the generator's output power. The steam turbine consists of six levels: axial steam flow direction type, single flow type, with a rotation speed of 3000 rpm, inlet steam pressure of 6.50 bar, and exit steam pressure of 0.15 bar. The results of the shaft modification show an increase in performance, producing an internal efficiency of 0.66 and a relative efficiency of 0.73 when the turbine operates with a steam volume of 144.46 kg/s. This turbine is suitable for production and operation because it meets the economic feasibility requirements with a Net Present Value of IDR 243,816,146,409,928.00 and an Internal Rate of Return of 58%. The payback period for the investment capital is 1.72 years. This research focuses on developing a turbine by analyzing its technological and economic aspects. The modifications include changes to the shaft and blade components. The number of blades affects the rotational speed, torque coefficient, power coefficient, and turbine efficiency.*

Keywords *- Balde, Geothermal power plant, Shaft, Steam, Turbine.*

1. Introduction

This energy source, geothermal, is non-polluting, inexpensive, and, in most cases, renewable, which makes it a promising source of power for the future [1]. The goal behind these new tables is not only to use them for the country update reports to the WGCs but mainly to build “a framework for geothermal data standards and methods to improve data collection to support the process of collecting, storing, and sharing coherent geothermal datasets” [2]. Electricity from geothermal sources represented more than 10% of the total generated in at least seven countries, led by Kenya, Iceland, and El Salvador. Practically all geothermal fields in operation are harnessing resources from hydrothermal, conventional reservoirs through an estimated 3700 production wells, with an annual average production of almost 3 MWh per well. This trend could continue in the next few years, but all can change due to the global urgency to maintain warming below the 1.5 °C threshold in the coming years [3]. A global suitability map would also support the understanding of the correlation between potential geothermal resource utilization and the sustainability of geothermal life cycles within the Life-Cycle Assessment (LCA) methodology [4]. The hydrothermal system, in contrast to the petrothermal system investigated, is found to meet several of the sustainability criteria examined (extraction equals recharge, operating lifetime of 100 to 300 years). However, economically optimal operation leads to excessive over-exploitation in both cases, showing a distinct trade-off between profit maximization and sustainable operation that has not been discussed in the literature so far [5]. Research on turbine shaft models was developed in Pro-E, and simulations were performed by applying boundary conditions as a fixed end to the ANSYS program and applying torque at 3000 rpm to the shaft at the other end [6]. The fatigue properties of the material used for the turbine shaft were 549.4 MPa - 3208.0 MPa [7]. The optimization outcomes indicate that reducing the vacuum pressure in the main condenser leads to enhanced exergy efficiency and increased power output. The optimal vacuum pressure obtained is 0.1 bar, resulting in the highest exergy efficiency and output power of 57.42% and 54,738 kW, respectively, with the lowest irreversibility of 32,751.07 kW [8]. Keeping the deflector plate on the upstream side of the blade will increase the efficiency of the turbine [9]. Based on the application of Capital Budgeting, methods commonly used to analyze an investment project include Net Present Value (NPV), Internal Rate of Return (IRR), and Payback Period (PP) [10].

1.1. Geothermal Systems

The Earth has three main layers: the crust, the mantle, and the core. These layers have different thicknesses and temperatures. The deeper the layer, the higher the temperature. At the top of the Earth's mantle, there is a lithosphere layer,

which is a thin and rigid plate. The plates move apart and push one another. Plates that push and plunge toward each other will experience a magnetization process. Hot rocks with low density will move upwards through the surrounding rock, causing heat transfer and an increase in temperature. Heat transfer occurs by conduction and convection. Conduction heat transfer occurs through rocks, and convection heat transfer occurs through rocks that contain water. Water's gravitational force tends to move downwards, but when it comes into contact with a heat source, the water temperature becomes higher and lighter. Hotter water will move upwards, and cooler water will move downwards to form circulation.

1.2. Hydrothermal Systems

Indonesia utilizes a hydrothermal system for its geothermal energy production. The hydrothermal system production process uses two wells: one for production and the other for injection [11-12]. Hot fluid is produced by drilling to a depth of less than 2 km. The production well is drilled across the reservoir to form a closed cycle, allowing the cold water pumped into the injection well to return to the surface through the production well after passing through the hot formation, which has fractures resulting from hydraulic fracturing. Failure of hydraulic fracturing can cause fluid loss during injection, disrupting the power plant's operation.

1.3. Utilization of Geothermal Energy for Generation

The geothermal fluid used for power generation has a temperature of more than 225˚C [13]. The properties of geothermal fluids are influenced by their natural characteristics, such as the presence of non-condensation gases, which cause scale formation and corrosion in pipes. As a result, geothermal power plants require more maintenance to ensure that the increasing partial pressure does not hamper the power produced by the turbine in the condenser. The geothermal fluid content for the West Java Mining Working Area (WKP) is a mixture of two phases, with the vapor phase being more dominant. Based on these conditions, the geothermal power generation method used is the single flash steam method with the following components: steam receiving header, separator, demister, turbine, generator, condenser, cooling tower, pump, and steam jet ejector.

2. Methods

2.1. Technological

Technological modification takes into account the following:

2.1.1. Shaft Power

Round shaft to transmit 55 MW power at 3000 rpm. The amount of planned power transmitted with an average power correction factor of 1.5, using the following equation [14]:

$$P_d = f_c \times P \quad (1)$$

P is the quotient of average power and mechanical efficiency. The Pd value is the nominal power output of the drive motor, and fc is the safety factor.

Table 1. Safety factor

Power Transmission	Safety factor
Average Power	1.2 – 2.0
Maximum power	0.8 – 1.2
Normal power	1.0 – 1.5

2.1.2. The magnitude of the twisting moment

The punter moment is calculated using the following equation [15]:

$$T = 9{,}74 \times 10^5 \frac{P_d}{n} \quad (2)$$

Where T is torsion moment [kg, mm], and n is rotational speed, [rpm].

2.1.3. Shear Stress

The turbine shaft is designed using AISI 4130 (American standard) or SCM2 (Japanese standard) material. The material's tensile strength is 85 kg/mm². The safety factor for SC materials, considering mass and alloy steel influence, is 6.0. The factor that influences stress concentration and surface roughness is 2.0 [16]. The permissible shear stress is:

$$\tau_a = \frac{\sigma_b}{Sf_1 \times Sf_2} \quad (3)$$

Where τa is shear stress, the guaranteed safety factor s_{f1} for SF material is 5.6, and for SC material is 6.0; s_{f2} is the roughness factor, with a value ranging from 1.3 to 3.3. σ_b is the material's tensile strength, which is 85 kg/mm².

2.1.4. Shaft Diameter

The shaft diameter with a torsion moment correction factor value of 1.2 and a bending factor of 1.0 is calculated using the following equation:

$$d_s = \left[\frac{5{,}1}{\tau_a} K_t C_b T\right]^{\frac{1}{3}} \quad (4)$$

Where d_s is the shaft diameter [mm], K_t is the torsion moment correction factor (1.2), and C_b is the bending factor (1.0).

2.1.5. Filet Fingers

The fillet radius with a diameter of the part containing the bearing of 360 mm is calculated as follows:

$$Filet\ fingers = \frac{360 - d_s}{2} \quad (5)$$

2.1.6. Stress Concentration in Stepped Shafts

The stress concentration in a stepped shaft is determined by the beta value, which represents the relationship between the fillet radius (r) divided by the shaft diameter (d_s) and the bearing ratio (D) divided by the shaft diameter (d_s).

2.1.7. Stress Concentration in Key-way Shafts

The stress concentration in a shaft with a key-way is determined by the alpha value, which represents the relationship between the fillet radius (r) divided by the shaft diameter (d_s).

2.1.8. Shear Stress

Shear stress with a shaft diameter of 350 mm is calculated as follows:

$$\tau = \frac{5{,}1T}{d_s^3} \quad (6)$$

Where τ is shear stress [kg/mm]

2.1.9. Conditions are considered successful if the shaft modification meets the following criteria

$$\tau_a \times \frac{Sf_2}{\alpha} > \tau \times C_b \times K_t \quad (7)$$

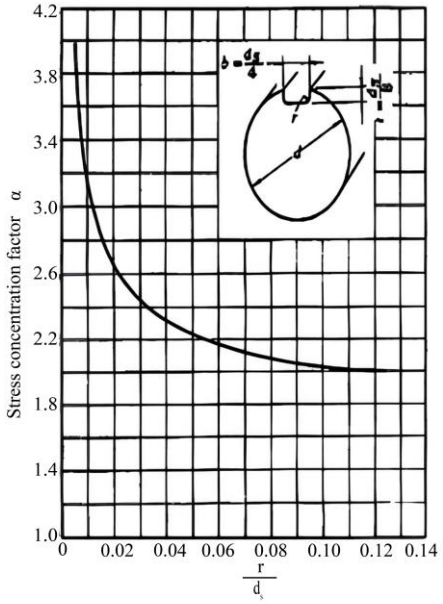

Fig. 1 Stress concentration factors (α) for statistical torque loading

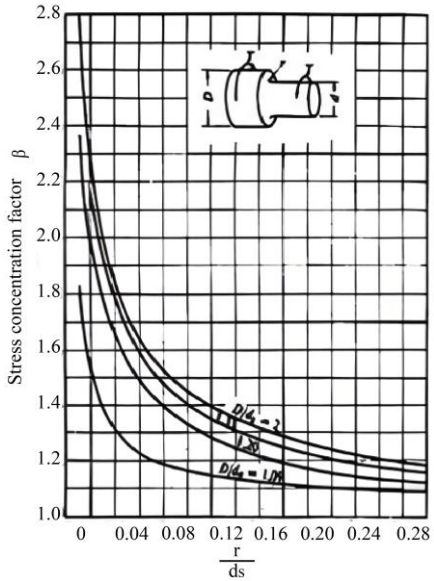

Fig. 2 Stress concentration factors (β) for statistical torque loading

2.2. Economic

2.2.1. Investment Costs

Investment costs include equipment costs, shipping costs, installation costs, contractor costs, and steam purchase costs. The equipment cost is predetermined based on the price of the turbine from Ruhn Power Ltd. Delivery cost calculations are detailed in calculation point 2. Installation and contractor costs are 50% and 10% of the equipment costs, respectively. The cost of purchasing steam per kWh is IDR 883.55. The following cost calculations are obtained [17]:

- Installation costs

  Installation costs = 50% × equipment costs (8)

- Contractor costs

  Contractor costs = 10% × equipment costs (9)

- Cost of purchasing steam

  Cost of buying steam = price of steam × shaftpowe (10)

2.2.2. Shipping Costs

Shipping costs include expedition costs, import duties, VAT, and PPH because they originate from China. The expedition fee is IDR 130,000,000.00, while the percentages for import duty VAT are 10%, 11%, and 7.5%, respectively, in accordance with the provisions of PMK No. 199 [18].

- Import duties

Entry fee = 10% x (expedition fee + equipment fee) (11)

- VAT

VAT = 11 % x (expedition fee + entry fee) (12)

- Income Tax

PPH = 7.5% x (expedition fee + entry fee) (13)

2.2.3. Engineering Economic Methods

- Turbine output costs

The conversion cost is equal to the cost per hour divided by the power generated.

Output costs are equal to the price of electricity minus conversion costs.

- Operation and maintenance costs

Maintenance costs are equal to the price of the electrical equipment multiplied by the power generated.

3. Results and Discussion

3.1. Analysis of Shaft Diameter

The steam will flow towards the moving blade, which will drive and rotate the shaft with the moving blade, resulting in a speed u. In order for the jet of steam coming out of the guide blade to function properly and without collision, it must have a ratio of c_1 and u, which has a relative efficiency value in the

maximum speed triangle. This can be depicted in a triangle of blade speed and angle and should be made as maximum as possible in variations 1 and 2 with varying values. The angle can be specified, but the magnitude of the angle is between (14^o to 20^o). The vapor velocity components depicted fall into the circumferential velocity directions cu and wu. The magnitude of these components serves to obtain the value of the tangential force generated by the steam flow when driving the turbine shaft. The value of the velocity component will be positive when in the direction of the turbine shaft and negative when opposite to the rotation of the turbine shaft. The turbine shaft transmits energy along with rotation. The shaft diameter design considers factors such as shaft strength, behavior, critical rotation, corrosion, and material. In generators, the turbine shaft carries high rotation and heavy loads, making alloy steel suitable. According to the American Standard, the chosen steel alloy is chromium molybdenum steel, specifically AISI 4130, to reduce maintenance. This research tests three materials: EN24 Stainless Steel, AISI 4130 Steel, and ZAMAK. The test results determine whether the AISI 4130 material has good performance against stress, vibration, and heat. The shaft diameter calculation begins with determining the design power and correction factors to meet the limit conditions. The power plant used as the basis for the calculation has a nominal power of 55 MW and an average power safety factor of 1.5. The SC material safety factor, considering mass and guide steel influence, is 6.0, and the stress concentration factor for surface roughness is 2.0. Therefore, the allowable shear stress is:

$$\tau_{allowable} = \frac{\sigma_b}{s_{f1} \times s_{f2}}$$

These values are then reviewed using ASME standard correction factors. The correction factor is determined to be 1.2, assuming the load is exposed to significant shock or impact. The calculation results show that the shaft diameter is 285 mm.

3.2. Blade Strength Analysis

The moving blade circumferential speed is an important modification parameter as it affects the speed triangle, losses, and main dimensions of the turbine. The moving blade circumferential speed is the moving blade circumferential speed plus the effect of the optimal value (u/c_1), which is determined based on the maximum relative efficiency of the speed triangle. The optimal value (u/c_1) with the relative efficiency value and the actual steam velocity leaving the fixed blade and this circumferential velocity will affect the moving blade circumferential velocity value, which is used to determine the disc diameter. The circumferential power (Pu) is the power at the turbine level, which is obtained from the product of the tangential force and the circumferential speed of the moving blade or rotor. In contrast, the relative efficiency of the velocity triangle is obtained from the quotient between the theoretical velocity of the steam leaving the nozzle and the sum of the absolute circumferential velocities of the moving blades. Results and discussion can be presented separately or in a combined section and can optionally be divided into major subsections. The analysis of blade strength against vibration aims to ensure that the designed turbine can operate safely and efficiently without experiencing damage due to excessive vibration. Vibrations in the turbine are divided into two types: free vibrations and forced vibrations.

Table 1. Specifications resulting from turbine shaft modifications

Parameter	Unit	Value
Material		AISI 4130
Tensile strength of materials	[kg/mm^2]	85
Shaft diameter	[mm]	350
Bearing diameter	[mm]	360

Table 2. Number of blades per level

Level	1	2	3	4	5	6
Fixed Blade	38	33	35	39	43	52
Moving Blade	43	38	39	43	50	61

Table 3. Number and height of fixed blades and moving blades for each level

Level	Unit	Fixed Blade			Moving Blade		
		Entry Side	Exit Side	Number of Blades	Entry Side	Exit Side	Number of Blades
1	[mm]	123	123	38	124	134	43
2	[mm]	188	200	33	210	248	38
3	[mm]	287	304	35	324	361	39
4	[mm]	366	397	39	438	446	43
5	[mm]	448	476	43	489	582	50
6	[mm]	742	871	52	949	1078	61

Table 4. Blade strength against vibration

Level	1	2	3	4	5	6
f_d(rps)	226.02	215.90	210.09	208.74	208.35	203.34

Table 5. Engineering economic methods [19]

Year	Investasi (Rp)	Power Generation	Electricity Price (Rp)	Electricity Sales (Rp)	Maintenance (Rp)	Cashflow (Rp)
0	-1,022,728,438,600.00					- 1,022,728,438,600.00
1		475,200,000	1,303.68	619,507,387,937.10	25,483,466,800.00	- 428,704,517,462.90
2		475,200,000	1,303.92	619,625,094,340.81	25,738,301,468.00	165,182,275,.409.91
3		475,200,000	1,304.17	619,742,823,108.73	25,995,684,482.68	758,929,414,035.97
4		475,200,000	1,304.42	619,860,574,245.13	26,255,641,327.51	1,352,534,346,953.58
5		475,200,000	1,304.67	619,978,347,754.23	26,518,197,740.78	1,945,994,496,967.03
6		475,200,000	1,304.92	620,096,143,640.31	26,783,379,718.19	2,539,307,260,889.15
7		475,200,000	1,305.16	620,213,961,907.60	27,051,213,515.37	3,132,470,009,281.37
8		475,200,000	1,305.41	620,331,802,560.36	27,321,725,650.53	3,725,480,086,191.21
9		475,200,000	1,305.66	620,449,665,602.85	27,594,942,907.03	4,318,334,808,887.02
10		475,200,000	1,305.91	620,567,551,039.31	27,870,892,336.10	4,911,031,467,590.23
11		475,200,000	1,306.16	620,685,458,874.01	28,149,601,259.46	5,503,567,325,204.77
12		475,200,000	1,306.40	620,803,389,111.19	28,431,097,272.06	6,095,939,617,043.91
13		475,200,000	1,306.65	620,921,341,755.12	28,715,408,244.78	6,688,145,550,554.25
14		475,200,000	1,306.90	621,039,316,810.06	29,002,562,327.22	7,280,182,305,037.09
15		475,200,000	1,307.15	621,157,314,280.25	29,292,587,950.50	7,872,047,031,366.84
16		475,200,000	1,307.40	621,275,334,169.96	29,585,513,830.00	8,463,736,851,706.80
17		475,200,000	1,307.65	621,393,376,483.46	29,881,368,968.30	9,055,248,859,221.96
18		475,200,000	1,307.89	621,511,441,224.99	30,180,182,657.99	9,646,580,117,788.96
19		475,200,000	1,308.14	621,629,528,398.82	30,481,984,484.56	10,237,727,661,703.20
20		475,200,000	1,308.39	621,747,638,009.22	30,786,804,329.41	10,828,688,495,383.00
21		475,200,000	1,308.64	621,865,770,060.44	31,094,672,372.70	11,419,459,593,070.80
22		475,200,000	1,308.89	621,983,924,556.75	31,405,619,096.43	12,010,037,898,531.10
23		475,200,000	1,309.14	622,102,101,502.42	31,719,675,287.40	12,600,420,324,746.10
24		475,200,000	1,309.39	622,220,300,901.70	32,036,872,040.27	13,190,603,753,607.50
25		475,200,000	1,309.63	622,338,522,758.87	32,357,240,760.67	13,780,585,035,605.70
26		475,200,000	1,309.88	622,456,767,078.20	32,680,813,168.28	14,370,360,989,515.60
27		475,200,000	1,310.13	622,575,033,863.94	33,007,621,299.96	14,959,928,402,079.60
28		475,200,000	1,310.38	622,693,323,120.38	33,337,697,512.96	15,549,284,027,687.00
29		475,200,000	1,310.63	622,811,634,851.77	33,671,074,488.09	16,138,424,588,050.70
30		475,200,000	1,310.88	622,929,969,062.30	34,007,785,232.97	16,727,346,771,880.10
Net Present Value						243,816,146,409,928.00
Internal Rate of Return						58%
Payback Period						1,72

Free vibrations occur due to the properties of the materials used, while forced vibrations occur due to periodic external influences. Under normal operating conditions, forced vibrations often occur due to the influence of steam flowing out of the fixed blade, causing the moving blade to vibrate. The turbine in this study was designed with a constant rotational speed of 3000 rpm or 50 Hz [20-22]. The success of the design is influenced by the analysis results based on static and dynamic frequency. Static frequency is the natural frequency of a structure in a stationary condition, while dynamic frequency pertains to a moving condition. The boundary condition that must be achieved so that the blade design can withstand vibrations is that the dynamic frequency calculated for each level is less than or equal to 350 Hz. The dynamic frequency of the design results can be seen in Table 4. Based on Table 4, the static frequency value for each level is constant because the design characteristics determine it. In contrast, the most significant dynamic frequency value occurs at the first level and decreases until the sixth level. The higher the turbine level, the smaller the amplitude of the vibrations produced due to the smaller energy transmitted to the turbine blades, which is proportional to the turbine pressure [23]. The analysis results show that the dynamic frequency value for each level is below the boundary conditions, indicating that the designed blade is safe and efficient to operate.

3.3. Economic Feasibility Analysis

The economic feasibility analysis identifies the viability of the design based on overall costs, from the design process to installation. The economic feasibility analysis was conducted using the Net Present Value (NPV), Payback Period (PBP), and Internal Rate of Return (IRR) methods [24]. If the values of these three methods meet the requirements, the design is considered feasible.

The designed turbine is planned to operate for 30 years. The output power produced by the turbine to drive the generator is 56,122.45 kW. The electrical energy produced by the generator is then sold to PLN to be distributed to consumers in Region 2 West Java. The economic feasibility of the design is based on the mechanical energy costs of the turbine output, derived from reducing the costs of selling electricity to PLN and converting it into electrical energy. The cost of electricity sales for a geothermal power plant (PLTP) with a capacity of 50 – 100 MW is IDR 1,313.28 per kWh (Presidential Decree 112 of 2022), while the cost of converting electrical energy is IDR 9.60 per kWh with a generator costing IDR 166,559,284,295.80, which operates for 36 years. The mechanical energy cost of the turbine output in the first year was IDR 1,303.68 per kWh. The cost increased yearly until it reached IDR 1,310.88 per kWh in the 30th year. The cost increase was due to the Electricity Price Inflation Rate of 0.02%, based on data from the Director-General of Electricity at the Ministry of Energy and Mineral Resources [25].

4. Conclusion

The modified blade can be deemed resistant to vibration if its dynamic frequency at each level is less than or equal to 350 rps. Furthermore, the steam turbine project is economically viable, evidenced by a Net Present Value (NPV) of IDR 243,816,146,409,928.00 and an Internal Rate of Return (IRR) of 58%. The investment capital is projected to be recouped in just 1.72 years, highlighting the project's financial feasibility.

Contributions

SW analyzed the data and wrote the manuscript, and SW and GIA conceived and designed the research. All authors have read and approved the manuscript.

References

[1] Moses Jeremiah Barasa Kabeyi, and Oludolapo Akanni Olanrewaju, "Geothermal Wellhead Technology Power Plants in Grid Electricity Generation: A Review," *Energy Strategy Reviews*, vol. 39, pp. 1-27, 2022. [CrossRef] [Google Scholar] [Publisher Link]

[2] Sheikh Muhammad Ali Haider et al., "Energy and Exergy Analysis of a Geothermal Sourced Multigeneration System for Sustainable City," *Energies*, vol. 16, no. 4, pp. 1-19, 2023. [CrossRef] [Google Scholar] [Publisher Link]

[3] Luis C.A. Gutiérrez-Negrín, "Evolution of Worldwide Geothermal Power 2020–2023," *Geothermal Energy*, vol. 12, no. 1, pp. 1-60, 2024. [CrossRef] [Google Scholar] [Publisher Link]

[4] Gianpaolo Coro, and Eugenio Trumpy, "Predicting Geographical Suitability of Geothermal Power Plants," *Journal of Cleaner Production*, vol. 267, pp. 1-11, 2020. [CrossRef] [Google Scholar] [Publisher Link]

[5] Fynn V. Hackstein, and Reinhard Madlener, "Sustainable Operation of Geothermal Power Plants: Why Economics Matters," *Geothermal Energy*, vol. 9, pp. 1-30, 2021. [CrossRef] [Google Scholar] [Publisher Link]

[6] Muhammad Sulman Kamboh, Mahtab Ali Machhi, and Muhammad Farhan Kamboh, "Design and Analysis of Drive Shaft with a Critical Review of Advance Composite Materials and the Root Causes of Shaft Failure," *International Research Journal of Engineering and Technology*, vol. 7, no. 6, pp. 3897- 3907, 2020. [Google Scholar] [Publisher Link]

[7] Bayu Rudiyanto, Arief Wicaksono, and Miftah Hijriawan, "Evaluation and Optimization Based on Exergy in Kamojan Geothermal Power Plant Unit 3," *International Journal on Advanced Science Engineering Information Technology*, vol. 13, no. 6, pp. 2372-2379, 2023. [CrossRef] [Google Scholar] [Publisher Link]

[8] Ji-Won Choi, Seung-Ho Han, and Kwon-Hee Lee, "Structural Analysis and Optimization of an Automotive Propeller Shaft," *Advances in Mechanical Engineering*, vol. 13, no. 10, 2021. [CrossRef] [Google Scholar] [Publisher Link]

[9] C.M. Shashikumar, and Vasudeva Madav, "Numerical and Experimental Investigation of Modified V-Shaped Turbine Blades for Hydrokinetic Energy Generation," *Renewable Energy*, vol. 177, pp. 1170–1197, 2021. [CrossRef] [Google Scholar] [Publisher Link]

[10] Ardyn Sari Sinaga et al., "Comparison of Capital Budgeting Methods: NPV, IRR, PAYBACK PERIOD," *World Journal of Advanced Research and Reviews*, vol. 19, no. 2, pp. 1078-1081, 2023. [CrossRef] [Google Scholar] [Publisher Link]

[11] Jian Wang et al., "Optimization of Large-Scale Daily Hydrothermal System Operations with Multiple Objectives," *Water Resources Research*, vol. 54, no. 4, pp. 2834–2850, 2018. [CrossRef] [Google Scholar] [Publisher Link]

[12] Scott Jess et al., "Determining the Lifespan of Hydrothermal Systems Using Thermochronology and Thermal Modeling," *Journal of Geophysical Research: Earth Surface*, vol. 126, no. 11, 2021. [CrossRef] [Google Scholar] [Publisher Link]

[13] Chijindu Ikechukwu Igwe, "Geothermal Energy: A Review," *International Journal of Engineering Research & Technology*, vol. 10, no. 3, pp. 655-661, 2021. [Google Scholar] [Publisher Link]

[14] Hilel Legmann, "The Bad Blumau Geothermal Project: A Low Temperature, Sustainable and Environmentally Benign Power Plant," *Geothermics*, vol. 32, no. 4-6, pp. 497–503, 2003. [CrossRef] [Google Scholar] [Publisher Link]

[15] Faisal Mahmuddin, "Rotor Blade Performance Analysis with Blade Element Momentum Theory," *Energy Procedia*, vol. 105, pp. 1123–1129, 2017. [CrossRef] [Google Scholar] [Publisher Link]

[16] Muaz Adnan et al., "Design, Analysis, and Fabrication of Water Turbine for Slow-Moving Water," *Journal of Energy Resources Technology*, vol. 144, no. 8, 2022. [CrossRef] [Google Scholar] [Publisher Link]

[17] John Messner, *Fundamentals of Building Construction Management*, The Pennsylvania State University, 2022. [Publisher Link]

[18] Rio Johan Putra, and Shiva Dewanti Nabila, "The Effect of VAT and Payroll Tax (Pph21) on the Growth of Community Consumption, Gross Domestic Product, and Economic Growth in Indonesia," *Journal Research of Social Science, Economics and Management*, vol. 1, no. 11, pp. 2016-2026, 2022. [CrossRef] [Google Scholar] [Publisher Link]

[19] Nurlaela Kumala Dewi, Riza Fathoni Ishak, and Afferdhy Ariffien, "Dry Port Financial Feasibility Analysis Model," *Journal of Innovation and Community Engagement*, vol. 5, no. 1, pp. 1-17, 2024. [CrossRef] [Google Scholar] [Publisher Link]

[20] Abdelrahman S. Abdeldayem et al., "Design of a 130 MW Axial Turbine Operating with a Supercritical Carbon Dioxide Mixture for the SCARABEUS Project," *International Journal of Turbomachinery Propulsion and Power*, vol. 9, no. 1, pp. 1-17, 2024. [CrossRef] [Google Scholar] [Publisher Link]

[21] Salma I. Salah, Martin T. White, and Abdulnaser I. Sayma, "A Comparison of Axial Turbine Loss Models for Air, sCO2 and ORC Turbines across a Range of Scales," *International Journal of Thermofluids*, vol. 15, pp. 1-22, 2022. [CrossRef] [Google Scholar] [Publisher Link]

[22] Emanuele Quaranta, "Optimal Rotational Speed of Kaplan and Francis Turbines with Focus on Low-Head Hydropower Applications and Dataset Collection," *Journal of Hydraulic Engineering*, vol. 145, no. 12, 2019. [CrossRef] [Google Scholar] [Publisher Link]

[23] Nancy Mauryaa et al., "Effect of Protuberances on the Aerodynamic Performance of a Wind Turbine Blade – A Review," *Energy Sources, Part A: Recovery, Utilization, and Environmental Effects*, vol. 46, no. 1, pp. 3416–3431, 2024. [CrossRef] [Google Scholar] [Publisher Link]

[24] Desi Harmada Wiratama, "Feasibility Analysis of Investment Assets for Business Development in The Calculation of Capital Budgeting in Surabaya UD Rahayu," *International Journal of Education and Social Science*, vol. 1, no. 1, pp. 16-27, 2020. [CrossRef] [Google Scholar] [Publisher Link]

[25] Jonathan A. Batten, Di Mo, and Armin Pourkhanali, "Can Inflation Predict Energy Price Volatility?," *Energy Economics*, vol. 129, pp. 1-18, 2024. [CrossRef] [Google Scholar] [Publisher Link]